

# Near Tip Measurement Issues in Cracked Bodies

C. W. SMITH

*Department of Engineering Science and Mechanics, Virginia  
Polytechnic Institute and State University Blacksburg,  
Virginia 2461, USA*

## ABSTRACT

From experimental results obtained over a period of approximately two years, the influence of side boundaries as well as free surfaces intersected by crack fronts on the location of the elastic linear zone (ELZ) dominated by the elastic stress singularity (or lowest or dominant eigenvalue) and the effect of embedded semi-rigid particles are quantified. These results suggest an interaction of the two types of boundary effects at a free surface and an outward movement of this zone in particulate composites.

## KEYWORDS

Crack tip analysis, Experimental measurements, Optical analysis, Dominant Eigenvalues, Stress Intensity Factors, Particulate effects.

## PREAMBLE

Using results from a series of near tip optical measurements on cracked bodies, this study attempts to quantify the influence on the size and location of the elastic linear zone (ELZ) of:

- i) External boundaries of plate surfaces (i.e. DE, DF, FG, EG in Fig. 1) hereafter called side boundaries.
- ii) Free surfaces intersected by crack fronts at right angles.
- iii) The presence of semi-rigid particles in a continuum matrix.

## SIDE BOUNDARY EFFECTS

While a substantial amount of literature exists on the influence of side boundaries upon the Stress Intensity Factor (SIF), their influence upon the size of the ELZ has received little attention. In order to focus attention upon this effect, we consider results from the following experiments. Test specimens of transparent polyurethane were prepared containing central cracks with the dimensions shown in Figure 1. The side boundaries of the large specimen were sufficiently far from the crack tip to exert only negligible influence upon the SIF there. The horizontal side boundaries of the small specimen were much closer to the crack tip than in the large specimen, but were still a respectable distance from the crack tip. The crack length was  $\approx 25$  mm. Through thickness photoelastic data for Mode I loading were taken (Fig. 2a), and SIF values were determined

using the two parameter ELZ algorithm [1]

$$\frac{K_{AP}}{\sigma(\pi a)^{1/2}} = \frac{K_1}{\sigma(\pi a)^{1/2}} + \frac{\sigma^0}{\sigma} \left(\frac{r}{a}\right)^{1/2} \quad (1)$$

where:

- $K_{AP} = \frac{nf}{2t} (8\pi r)^{1/2}$   $n$  = photoelastic stress fringe order  
 $f$  = photoelastic material fringe value  
 $t$  = specimen thickness  
 $r$  = distance from crack tip normal to crack plane  
 $K_1$  = SIF  
 $\frac{K_1}{\sigma}$  = Remote uniform stress normal to crack plane  
 $\sigma^0$  = non-singular constant normal stress parallel to crack plane  
 $a$  = half crack length

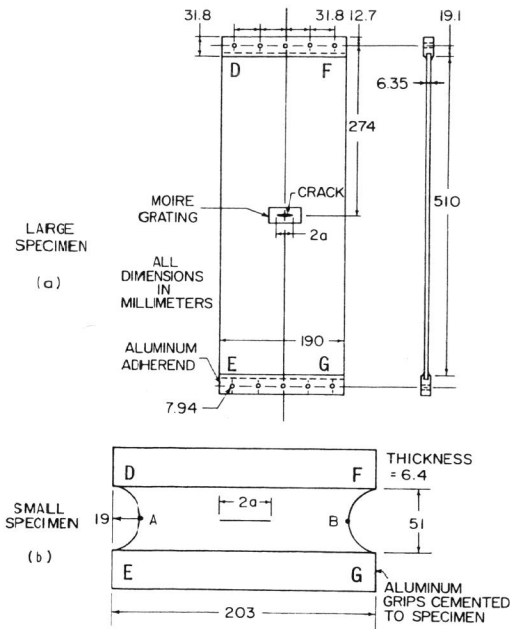


Fig. 1 Dimensions of Test Specimens

A typical result using Eq. (1) on test data from a large specimen is shown in Fig. 3. SIF values compared favorably with analytical results given in Ref. [2], implying that the value of the stress singularity ( $\lambda$ ) was, indeed  $1/2$ . The ELZ's revealed by the test data showed a constiction of the size of that zone measured normal to and from the crack

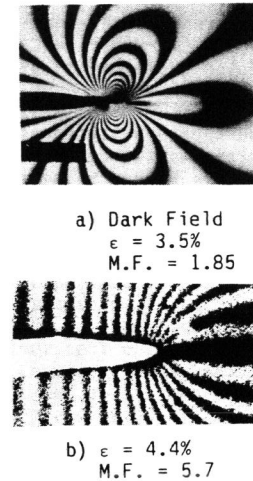


Fig. 2 Photoelastic and Moire Fringe Patterns from Small Polyurethane Specimens

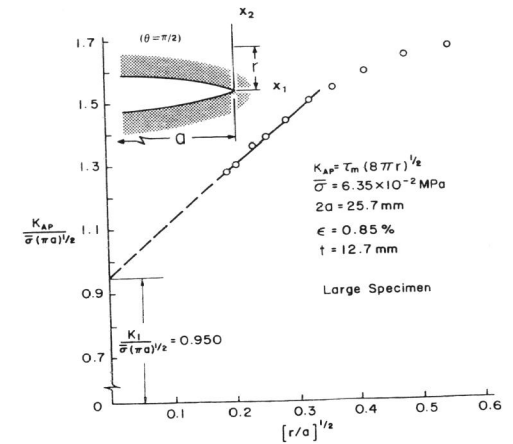


Fig. 3 Determination of SIF ( $\lambda_\sigma = 1/2$ , LEFM)

tip of from 1.0 to 3.0 mm in the large specimen to 0.7 to 2.0 mm in the smaller one. When normalized with respect to the crack length, and reported as  $(r/a)^{1/2}$ , values were 0.28 to 0.48 and 0.22 to 0.33, respectively. A survey of the application of photoelastic methods to SIF determination is given in Ref. [3].

#### FREE SURFACE EFFECTS

Using the same specimens described above, a moire grating of 20 lines/mm was attached to a free surface over one crack tip in each of the specimens pictured in Fig. 1 and the specimens were reloaded and viewed through a master grating of the same line density to obtain the moire pattern for the displacement component normal to the crack plane (Fig. 2b). Then, using the variable singularity order algorithm [4],

$$\log u_2 = \log D_2 + \lambda_u \log r \quad (2)^*$$

where  $u_2$  = displacement component normal to the crack and  $\lambda_u$  is the dominant eigenvalue or lowest order singularity. (The moire fringe order is proportional to  $u_2$ .) An example of the use of this algorithm in determining  $\lambda_u$  is shown in Fig. 4. The order of the dominant displacement eigenvalue  $\lambda_u$  was found to be  $\approx 0.69$  (or  $\lambda_\sigma \approx 0.31$ ) which was quite close

\* All logs are natural logs

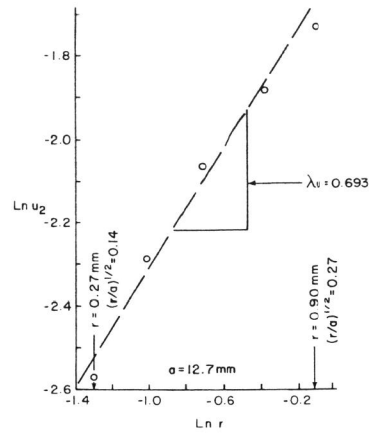


Fig. 4 Determination of  $\lambda_u$  at Free Surface for Small Polyurethane Specimen

to the results obtained in Refs. [4] and [5]. Moreover, data plots revealed the presence of a strong further constriction of the ELZ. The results are summarized in Table I and represent averages from several tests. Details of use of the Moire Method in near tip measurements are found in Ref. [1]. These results may be interpreted in the following way. The photoelastic results reveal the ELZ constriction due to the horizontal side boundaries only while the moire results capture the combined effects of the side boundaries and the free surface effect. For the large specimen, the constriction of the ELZ at the free surface is significantly less than for the small specimen, suggesting the presence of a strong interaction between the side boundaries and the free surface in the small specimens.

Table I  
Location of ELZ in Terms of  $(r/a)^{1/2}$  Values

	Large Specimen	Small Specimen
Photoelastic	0.28 to 0.48	0.22 to 0.33
Moire	0.17 to 0.53	0.14 to 0.27

#### EXTENSION TO POLYPHASE MATERIALS

In recent years, considerable interest has been directed towards the use of particulate composite materials for a variety of applications. In such materials, at least two distinct phases exist. The first is a matrix and the second consists of particles embedded in the matrix. When the matrix of the composite is nearly incompressible, then it is not unlikely that a free surface effect such as described in the foregoing may exist where a crack in the matrix intersects a free surface of the composite. As a result of the success achieved in measuring these effects in continua, it was decided to attempt to extend them to a study of free surface effects in a particulate composite.

The composite chosen consisted of a soft rubber matrix somewhat similar to polyurethane containing embedded semi-rigid polyhedral crystals which ranged in size from 10 to 500 microns (i.e. 0.01 to 0.50 mm). The focus of the study was to determine if the methods and algorithms used on the continuum-like polyurethane material could be applied to a study of such a composite. Preliminary studies suggested that the surface properties of the composite might be better suited to a mechanical grating analysis than to moire and that the algorithm employed for the displacements should be modified to account for some rather severe blunting

observed at the crack tip. The modified form of Eq. 2 was

$$\log(u_2 - u_{20}) = \log D_2 + \lambda_u \log r \quad (3)$$

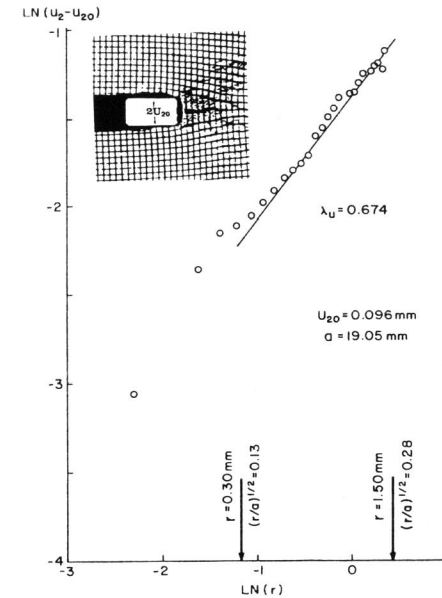


Fig. 5 Determination of  $\lambda_u$  for a Particulate Composite Specimen

A typical set of data for  $u_2$  determination showing the  $u_{20}$  measurement is shown in Fig. 5. Using a grating made by placing a screen on the specimen surface and applying either titanium dioxide powder or evaporated aluminum, after which the screen was removed, gratings of 5 and 20 lines/mm were formed over one crack tip on the free surface of specimens having the dimensions shown in Fig. 1b (i.e. the small specimen). The near tip region was then photographed at various stages of crack opening and growth. A sequence of such photographs are shown in Fig. 6. These observations, when compared with the crack opening and growth in polyurethane, show a blunter crack tip with a craze or damage zone ahead of it during crack opening which was not observed in the polyurethane, and a very irregular crack profile as it joins with voids ahead of the crack during extension. The blunting is believed to result from the craze zone which develops ahead of the crack due to the larger semi-rigid particles being pulled apart leaving a

matrix rich craze zone. The irregular nature of the crack tip profile during growth is likely due to the random size and distribution of the semi-rigid particles and zones of dewetting. From a study of several such crack tip profiles, it was concluded that it would only be feasible to accurately measure values of  $\lambda_u$  during the crack opening stage. Such measurements were made in a series of tests and results are reported in Table II. While  $\lambda_u$  values are similar to the polyurethane tests,

Table II  
Average Values of  $\lambda_u$  During Crack Opening  
Global Strain Range 1.25 to 10.00%

Test No.	$(\lambda_u)_{AVG}$	Location of ELZ in Terms of $(r/a)^{1/2}$ Values
1	0.71	$[(r/a)^{1/2}]_{range} = 0.50 \text{ to } 2.00$ $[(r/a)^{1/2}]_{AVG} = 0.70 \text{ to } 1.50$
2	0.69	
3	0.69	
4	0.66	

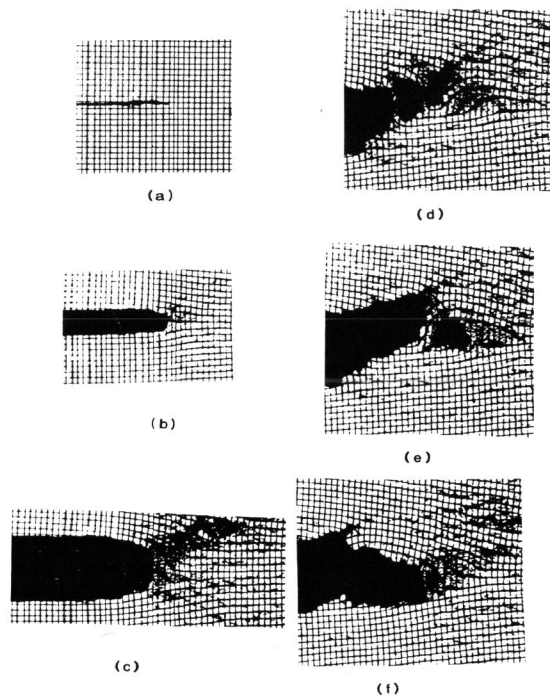


Fig. 6 Crack Opening and Growth in a Particulate Composite

comparison between Tables I and II shows an outward movement of the ELZ for the composite material. The outward movement of the data zone here relative to its location in the polyurethane is likely due to the blunting effect resulting from the presence of the rigid particles.

#### SUMMARY

Results from studies by the author and his colleagues spanning approximately two years have been used to demonstrate the influence of side boundaries, free surfaces, embedded particles and their interactions upon the location of the elastic linear zone used in the determination of fracture parameters. It is believed that these effects merit special consideration especially when making surface measurements on nearly

incompressible materials. Attempts to extend these studies to growing cracks are continuing.

#### ACKNOWLEDGEMENTS

The author wishes to acknowledge the contributions of R. W. Lloyd, M. Rezvani, C. W. Chang, R. Czarnek and D. Post for their contributions to parts of the above studies. Also the advice of C. T. Liu and the support of the U.S. Astronautics Laboratory under Contracts No. F04611-85-C0098 and F0-4611-87-C-0057 are gratefully acknowledged.

#### REFERENCES

- [1] Smith, C. W. and Kobayashi, A. S., (1987). Experimental fracture mechanics, Ch. 20 of Handbook on Experimental Mechanics, Society for Experimental Mechanics.
- [2] Rooke, D. P. and Cartwright, D. J., (1976). Compendium of stress intensity factors, Her Majesty's Stationary Office, London.
- [3] Østervig, Carl B., (1987). Stress intensity factor determination from isochromatic fringe patterns - a review, Journal of Engineering Fracture Mechanics, Vol. 26, No. 6, pp. 937-944.
- [4] Benthem, J. P., (1980). The quarter infinite crack in a half space: alternative and additional solutions, International Journal of Solids & Structures, Vol. 16, pp. 119-130.
- [5] Smith, C. W. and Epstein, J. S., (1984). Measurement of three dimensional effects in cracked bodies, Proc. of International Congress on Experimental Mechanics, pp. 102-110.